environmental microbiology

Environmental Microbiology (2017) **19**(5), 1959–1974 doi:10.1111/1462-2920.13710

MST50 is involved in multiple MAP kinase signaling pathways in *Magnaporthe oryzae*

Guotian Li,[1,2†] Xue Zhang,[2†] Huan Tian,[1] Yoon-E Choi,[3] W. Andy Tao[4] and Jin-Rong Xu[1,2*]

[1]*Purdue-NWAFU Joint Research Center, College of Plant Protection, Northwest A&F University, Yangling, Shaanxi 712100, China.*

[2]*Department of Botany and Plant Pathology, Purdue University, West Lafayette, IN, 47907, USA.*

[3]*Division of Environmental Science and Ecological Engineering, College of Life Sciences and Biotechnology, Korea University, Seoul, 136-713, Republic of Korea.*

[4]*Department of Biochemistry, Purdue University, West Lafayette, IN 47907, USA.*

Summary

Appressorium formation plays a critical role in *Magnaporthe oryzae*. Mst50 is an adapter protein of the Mst11-Mst7-Pmk1 cascade that is essential for appressorium formation. To further characterize its functions, affinity purification was used to identify Mst50-interacting proteins (MIPs) in this study. Two of the MIPs are Mst11 and Mst7 that are known to interact with Mst50 for Pmk1 activation. Surprisingly, two other MIPs are Mck1 and Mkk2 that are the upstream kinases of the Mps1 pathway. Domain deletion analysis showed that the sterile alpha-motif of Mst50 but not the Ras-association domain was important for its interaction with Mck1 and responses to cell wall and oxidative stresses. The *mst50* mutant was reduced in Mps1 activation under stress conditions. *MIP11* encodes a RACK1 protein that also interacted with Mck1. Deletion of *MIP11* resulted in defects in cell wall integrity, Mps1 phosphorylation and plant infection. Furthermore, Mst50 interacted with histidine kinase Hik1, and the *mst50* mutant was reduced in Osm1 phosphorylation. These results indicated that Mst50 is involved in all three MAPK pathways in *M. oryzae* although its functions differ in each pathway. Several MIPs are conserved hypothetical proteins and may be involved in responses to various signals and crosstalk among signaling pathways.

Received 8 December, 2016; revised 17 February, 2017; accepted 19 February, 2017. *For correspondence: E-mail: jinrong@purdue.edu; Tel. 765-496-6918; Fax 765-496-6918. †These two authors contributed equally.

Introduction

Magnaporthe oryzae, a hemibiotrophic filamentous fungus, is the causal agent of rice blast, which is one of the most devastating diseases of rice worldwide (Dean *et al*., 2005; Wilson and Talbot, 2009). The fungus infects plants in a manner typical of many foliar pathogens by the differentiation of dome-shaped infection structures called appressoria. The enormous turgor pressure accumulated in melanized appressoria is used to penetrate plant cuticle and cell wall (Howard *et al*., 1991; Thines *et al*., 2000). After penetration, invasive hyphae initially grow biotrophically in plant cells (Kankanala *et al*., 2007; Mosquera *et al*., 2009). Various fungal effectors have been identified to play important roles during invasive growth (Mentlak *et al*., 2012; Chen *et al*., 2014). Whereas the biotrophic interfacial complex is important for the translocation of cytoplasmic effectors, apoplastic effectors are secreted from invasive hyphae via the conventional secretory pathway (Giraldo *et al*., 2013; Zhang and Xu, 2014).

In the past two decades, a number of well conserved signal transduction pathways, including three MAP kinase (MAPK) and the cAMP-PKA pathways, have been shown to regulate appressorium formation, penetration and other infection processes in *M. oryzae*. Appressorium formation can be induced by the attachment of germ tubes to hydrophobic surfaces in the rice blast fungus, and surface recognition is known to be mediated by the cAMP-PKA pathway formation (Mitchell and Dean, 1995; Xu *et al*., 1997). Several components of the cAMP-PKA pathway have been functionally characterized in *M. oryzae*, including *MAC1, CPKA, SUM1* and *CAP1* (Lee and Dean, 1993; Mitchell and Dean, 1995; Choi and Dean, 1997; Zhou *et al*., 2012). *MAC1* encodes an adenylate cyclase that is important for aerial hyphal growth, conidiation, appressorium formation and plant infection (Choi and Dean, 1997). Deletion of the *CPKA* catalytic subunit of PKA results in a delay in appressorium formation and defects in appressorium penetration (Mitchell and Dean, 1995; Xu *et al*., 1997).

Although it is not involved in surface recognition, the Pmk1 MAPK pathway is essential for appressorium formation and invasive growth. The *pmk1* mutant fails to form appressoria and is nonpathogenic on either intact or wounded rice leaves (Xu and Hamer, 1996). Several components of the Pmk1 pathway have been characterized, including *MST11*, *MST7*, *MST50*, *MoMSB2*, *MST12* and *MoSFL1* (Park *et al*., 2002; Zhao *et al*., 2005; Park *et al*., 2006; Liu *et al*., 2011; Li *et al*., 2012). Mst7 and Mst11 are the MAPK kinase (MEK) and MEK kinase (MEKK), respectively, that function upstream from Pmk1 (Zhao *et al*., 2005). The *mst11* and *mst7* mutants have the same defects in appressorium formation and plant infection as the *pmk1* mutant. *RAS2* is an essential gene and it appears to function upstream from both cAMP-PKA and Pmk1 MAPK pathways. Expressing a dominant active *RAS2* allele over-activated both Pmk1 and PKA and resulted in the formation of appressorium-like structures without surface attachment (Park *et al*., 2006; Zhou *et al*., 2014). For the other two MAPK genes in *M. oryzae*, *MPS1* is important for cell wall integrity, conidiogenesis and plant infection (Xu *et al*., 1998) but *OSM1* is dispensable for virulence although it has the conserved function in osmoregulation (Dixon *et al*., 1999). The *mps1* deletion mutant is defective in appressorium penetration and has autolysis defect with its aerial hyphae. Mck1 and Mkk2 are the MEKK and MEK functioning upstream from Mps1. The *mck1* mutant phenocopies the *mps1* mutant in hyphal autolysis, rare conidiation and loss of virulence (Jeon *et al*., 2008).

Mst50 is an essential component of the Pmk1 pathway, functioning as an adaptor protein tethering together Mst11 and Mst7 (Zhao *et al*., 2005; Park *et al*., 2006). Deletion of *MST50* abolishes Pmk1 phosphorylation and the *mst50* mutant has similar defects to the *pmk1* mutant in appressorium formation and nonpathogenic. The sterile alpha-motif (SAM) domain of Mst50, but not its Ras-association domain (RAD), is essential for appressorium formation and its interaction with Mst11 (Park *et al*., 2006). Orthologues of Mst50 also have been shown to be essential for infection and other developmental process in several fungal pathogens, including *Zymoseptoria tritici* (Kramer *et al*., 2009), *Botrytis cinerea* (Schamber *et al*., 2010), *Ustilago maydis* (Mayorga and Gold, 2001) and the human pathogen *Cryptococcus neoformans* (Fu *et al*., 2011). In *Saccharomyces cerevisiae*, Ste50 is involved in mating, invasive or filamentous growth, and the Sho1-dependent response to hyperosmolality (Jansen *et al*., 2001; Ramezani-Rad, 2003; Kwan *et al*., 2006; Truckses *et al*., 2006). In *M. oryzae*, Mst50 also was shown to interact with Ras proteins, Cdc42 and Mgb1 (Park *et al*., 2006), indicating that Mst50 may play a critical role in interacting with other components of the Pmk1 pathway and it may be involved in other signaling pathways.

To further characterize the functions of Mst50, we used the affinity purification approach to identify Mst50-interacting proteins (MIPs) in *M. oryzae*. In addition to proteins known to interact with Mst50, we identified 18 other putative MIPs in this study. Three of the MIPs confirmed by co-immunoprecipitation (co-IP) assays are components of the Mps1 and Osm1 MAPK pathways that are important for responses to cell wall, oxidative and hyperosmotic stresses (Motoyama *et al*., 2005; Jeon *et al*., 2008; Yin *et al*., 2015). Mip11 is a RACK1 protein that also interacted with Mck1, and the *mip11* mutant was defective in plant infection. These results indicated that Mst50 is involved in all three MAP kinase pathways in *M. oryzae* although the importance and functions of Mst50 in each pathway are different. Furthermore, several MIPs are conserved in filamentous ascomycetes but lack distinct orthologues in the budding yeast. Some of them may be important for proper responses to various external stresses or signals and crosstalk among these different signaling pathways in *M. oryzae*.

Results

Identification of proteins associated with Mst50 in vivo

To identify Mst50-interacting proteins, we generated an Mst50-3xFLAG construct and transformed it into the *mst50* mutant. The resulting transformant HZ115 (Table 1) was rescued in appressorium formation and plant infection (Supporting Information Fig. S1), indicating that the Mst50-3xFLAG construct was fully functional. To minimize the background difference, we transformed the Mst50-3xFLAG fusion into the wild-type strain 70-15 as HZ112 (Table 1). Mst50-interacting proteins were purified from total proteins isolated from transformant HZ112 with anti-FLAG M2 beads and identified by mass spectrometry analysis (Ding *et al*., 2010).

Mst50-interacting proteins (MIPs) that were co-purified with Mst50 were listed in Table 2. Two of them were the MEK (Mst7) and MEKK (Mst11) of the Pmk1 MAPK pathway. In *M. oryzae*, Mst11 and Mst7 are known to interact with Mst50 in yeast two-hybrid and co-immunoprecipitation (co-IP) assays (Zhao *et al*., 2005;). Mip3 is the Chm1 PAK kinase that is important for appressorium morphogenesis and penetration (Li *et al*., 2004). Interestingly, several MIPs were components of the Mps1 MAPK pathway, including Mck1 (Mip4), Mkk2 (Mip5) and Mip6. Mck1 and Mkk2 are the MEKK and MEK that activate the Mps1 MAPK in *M. oryzae* (Jeon *et al*., 2008). Mip6 is orthologous to the yeast Rho1 small GTPase that functions upstream of the Slt2 pathway (Levin, 2011). In addition, Mip7 (Hik1 histidine kinase) is the osmosensor that is involved in Osm1 phosphorylation in *M. oryzae* (Motoyama *et al*., 2005). Other proteins that co-purified with Mst50 included the Rack1 orthologue Mip11 (Adams *et al*., 2011), one putative

Table 1. Wild-type and mutant strains of *Magnaporthe oryzae* used in this study.

Strain	Genotype description	Reference
70-15	Wild type (*MAT1-1*)	(Chao and Ellingboe, 1991)
Guy11	Wild type (*MAT1-2*)	(Chao and Ellingboe, 1991)
Ku80	*ku80* deletion mutant of Guy11	(Villalba *et al*., 2008)
MF103	*mst50* deletion mutant	Park *et al*. (2006)
HZ115	Transformant of MF103 expressing Mst50-3xFLAG	This study
HZ112	Transformant of 70-15 expressing Mst50-3xFLAG	This study
LA24	Transformant of 70-15 expressing Chm1-3xFLAG	This study
LA35	Transformant of 70-15 expressing Chm1-3xFLAG	This study
YE8	Transformant of 70-15 expressing Mck1-3xFLAG	This study
GT24	Transformant of 70-15 expressing Mip13-3xFLAG	This study
GT88	Transformant of 70-15 expressing Mip14-3xFLAG	This study
YE5	Transformant of 70-15 expressing Mip17-3xFLAG	This study
YE26	Transformant of 70-15 expressing Mip18-3xFLAG	This study
ms85	*mst20* deletion mutant	Li *et al*. (2004)
MC55	*chm1* deletion mutant	Li *et al*. (2004)
nn78	*pmk1* deletion mutant	(Xu and Hamer, 1996)
M3H51	*mps1* deletion mutant	Xu *et al*. (1998)
JH73	*osm1* deletion mutant	Dixon *et al*. (1999)
CMF11	MF103 transformed with the wild-type *MST50* allele	Park *et al*. (2006)
SD1	$MST50^{\Delta SAM}$ in MF103	Park *et al*. (2006)
RD1	$MST50^{\Delta RAD}$ in MF103	Park *et al*. (2006)
Bk5	*mck1* deletion mutant	This study
Bk7	*mck1* deletion mutant	This study
Rk17	*mip11* deletion mutant	This study
Rk26	*mip11* deletion mutant	This study
RkC18	Transformant of Rk26 expressing Mip11-GFP fusion	This study
Gk5	*mip17* deletion mutant	This study
Gk7	*mip17* deletion mutant	This study

Table 2. Putative Mst50-interacting proteins identified by affinity purification.

Name	Gene ID	Predicted functions
Mst50	MGG_05199.6	Mst50 adaptor protein
Mip1[a]	MGG_14847.6	Mst11 MEK kinase
Mip2[a]	MGG_00800.6	Mst7 MEK
Mip3[b]	MGG_06320.6	p21-activated kinase, Chm1
Mip4[b,c]	MGG_00883.6	Mck1 MEK kinase
Mip5[c]	MGG_06482.6	Mkk2 MEK
Mip6	MGG_07176.6	Rho1 GTPase
Mip7	MGG_11174.6	Hik1 histidine kinase
Mip8	MGG_06496.6	G protein effector, homologous to yeast Scp160
Mip9	MGG_02696.6	Woronin body major protein
Mip10	MGG_12814.6	bZip transcription factor
Mip11[b]	MGG_04719.6	WD40 repeat-containing protein orthologous to RACK1
Mip12	MGG_03838.6	Ser/Thr protein phosphatase family protein
Mip13[b]	MGG_02405.6	G2/M phase checkpoint control protein Sum2
Mip14[b]	MGG_08820.6	Putative cargo-transport protein
Mip15	MGG_04752.6	Atp4 ATP synthase
Mip16	MGG_08015.6	Conserved C2H2 finger domain-containing protein
Mip17[b]	MGG_05752.6	Conserved hypothetical protein
Mip18	MGG_03663.6	Conserved hypothetical protein
Mip19	MGG_01101.6	Conserved hypothetical protein
Mip20	MGG_13743.6	Conserved ankyrin repeat-containing protein

a. Interaction with Mst50 was confirmed by co-IP and/or yeast two-hybrid assays in previous studies.
b. Interaction with Mst50 was confirmed by co-IP assays in this study.
c. Interaction with Mst50 was confirmed by yeast two-hybrid assays in this study.

serine/threonine protein phosphatase PP2A (Mip12), one G protein effector (Mip8), and several conserved hypothetical proteins (Mip16-Mip20) (Table 2). These results indicate that Mst50 may be involved in multiple signaling pathways in *M. oryzae*.

Verification of Mst50-interacting proteins by co-IP assays

To confirm the interaction of MIPs with Mst50, we generated a rabbit antibody with the Mst50-specific oligo-peptide AEASPTESDPPSNEC. The resulting anti-Mst50 antibody detected a 52-kDa band in the wild-type strain (Supporting Information Fig. S2), which is the predicted size of Mst50. The same band was not detectable in the *mst50* mutant (Supporting Information Fig. S2), indicating that this antibody is suitable for Mst50 detection.

We then generated 3xFLAG fusion constructs for six selected MIPs and transformed them into the wild-type strain 70-15. The resulting hygromycin-resistant transformants were screened by PCR and further examined by western blot analysis with the anti-FLAG antibody. Total proteins isolated from transformants expressing these 3xFLAG fusion constructs (Table 1) were then incubated with anti-FLAG M2 beads. After three washes, proteins bound to anti-FLAG beads were eluted and subjected to western blot analysis. The Mst50 band was detected in proteins eluted from anti-FLAG beads of the five transformants expressing the Chm1-, Mck1-, Mip13-, Mip14- and Mip17-3xFLAG fusion proteins but not the three transformants expressing the Mip18-3xFLAG fusion protein (Fig. 1). Co-IP assays confirmed that these five proteins interact with Mst50 in *M. oryzae*.

Chm1 is not important for Pmk1 activation

To our surprise, one of the Mst50-interacting proteins is Chm1 (Li *et al*., 2004). The interaction between Chm1 and Mst50 was confirmed by co-IP assays (Fig. 1). Although the PAK kinase, Ste20, plays a critical role in the activation of the pheromone response pathway in *S. cerevisiae*, its orthologue is dispensable for appressorium formation in *M. oryzae* (Li *et al*., 2004). Chm1 is the other PAK kinase in the rice blast fungus and the *chm1* mutant has pleiotropic defects, including abnormal appressorium morphology and loss of pathogenicity (Li *et al*., 2004). To determine whether the interaction of Chm1 with Mst50 plays a direct role in Pmk1 activation, we assayed the phosphorylation level of Pmk1 with an anti-TpEY antibody. In comparison with the wild type, the phosphorylation level of Pmk1 was not significantly affected in the *chm1* mutant (Supporting Information Fig. S3), indicating that Chm1 plays no or only a minor role in Pmk1 activation.

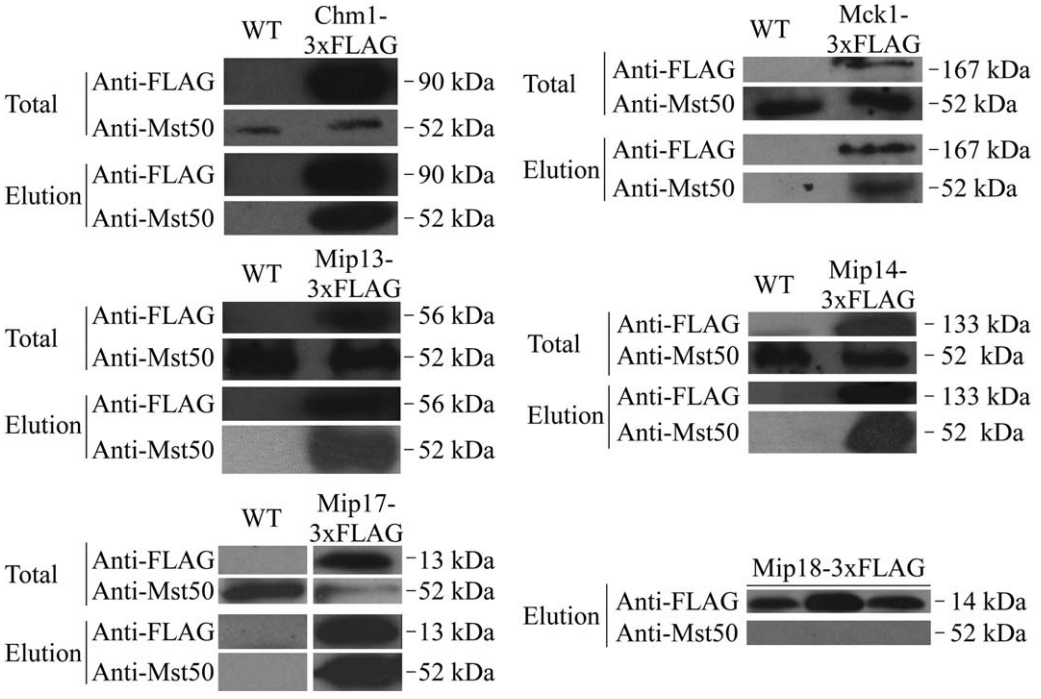

Fig. 1. Co-immunoprecipitation assays with Chm1, Mck1, Mip13, Mip14, Mip17 and Mip18.
Western blots of total proteins (total) and proteins eluted from anti-FLAG M2 beads (elution) of the wild-type strain 70-15 (WT) and transformants expressing the 3xFLAG fusion construct of the marked genes were probed with the anti-FLAG and anti-Mst50 antibodies. The Mst50 band of the expected size (labelled on the right) was only detected in eluates of the Chm1-, Mck1-, Mip13-, Mip14- and Mip17-3xFLAG transformants.

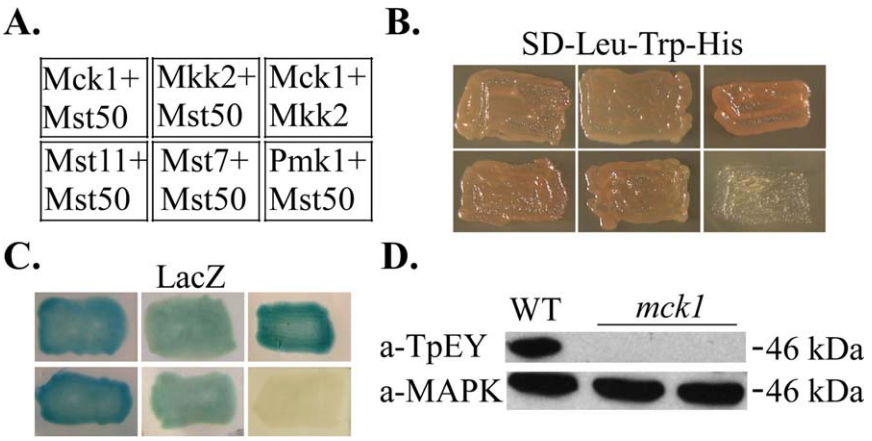

Fig. 2. Yeast two-hybrid assays for the interactions of Mst50 with different MIPs and TEY phosphorylation assays with the *mck1* mutant.
A. Diagram for yeast transformants used for yeast two-hybrid assays.
B and **C**. Yeast transformants expressing the marked bait and prey constructs were assayed for growth on SD-Leu-Trp-His (SD-His) and β-galactosidase activities (LacZ).
D. TEY phosphorylation assays with the *mck1* deletion mutant. Western blots of proteins isolated from vegetative hyphae of the wild-type strain 70-15 (WT) and *mck1* mutants Bk5 and Bk7 were probed with the anti-MAPK and anti-TpEY antibodies for the expression and phosphorylation levels of Mps1 (46 kDa) respectively. [Colour figure can be viewed at wileyonlinelibrary.com]

Mst50 interacts with Mck1 and Mkk2

In addition to co-IP assays (Fig. 1), we verified the direct interaction between Mst50 and Mck1 by yeast two-hybrid assays. The Mck1 bait construct was generated and co-transformed with the Mst50 prey construct into yeast strain YRG-2 (Zhao *et al*., 2005). The resulting transformants were able to grow on SD-Leu-Trp-His (SD-His) plates and had strong LacZ activities (Fig. 2), indicating the direct interaction between Mck1 and Mst50.

We also examined the interaction of Mst50 with Mkk2 by yeast two-hybrid assays (Fig. 2A). In comparison with the Mck1-Mst50 interaction, the interaction between Mkk2 and Mst50 was weaker (Fig. 2B and C). These results indicate that Mst50 may directly interact with both Mck1 and Mkk2, the putative MEKK and MEK that activate Mps1. In this study, we generated the *mck1* null mutant of strain Ku80 (Villalba *et al*., 2008) and found that it had similar defects in cell wall integrity, conidiation and pathogenesis (Supporting Information Fig. S4) to the *mck1* mutant of strain KJ201 (Jeon *et al*., 2008). When assayed with an anti-TpEY antibody, the phosphorylation of Mps1 was abolished in the *mck1* deletion mutant (Fig. 2D), confirming the essential role of Mck1 in the activation of Mps1 in *M. oryzae*.

Mst50 plays a role in the activation of Mps1 in response to cell wall stress

The *mst50* mutant is known to have increased sensitivity to cell wall-degrading enzymes (Park *et al*., 2006). Because of the interaction of Mst50 with Mck1 and Mkk2, we assayed the cell wall integrity defects of the *mst50* mutant. In the presence of 50 μg/ml Calcofluor white (CFW), approximately 99% of conidia germinated after incubation at room temperature for 6 h in the wild-type strain 70-15. Under the same conditions, only approximately 5% of the *mst50* mutant conidia produced germ tubes (Fig. 3A) and the *mps1* mutant failed to germinate. Without CFW, conidia of the *mst50* and *mps1* mutants germinated as efficiently as the wild-type strain.

To further confirm the role of *MST50* in the cell wall integrity pathway, we assayed the activation of Mps1 in

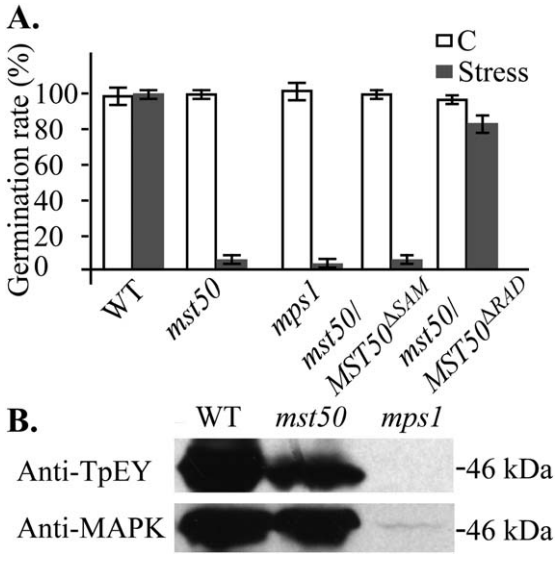

Fig. 3. Assays for increased sensitivity of the *mst50* mutant to cell wall stress.
A. Conidium germination assays. Conidium suspensions of the wild-type strain 70-15 (WT), *mst50* (MF103), *mps1* (M3H51) and MF103 transformants expressing different *MST50* alleles SD1 (*mst50*/*MST50*$^{\Delta SAM}$) and RD1 (*mst50*/*MST50*$^{\Delta RAD}$) were inoculated on plastic cover slips with (grey columns; Stress) or without (white columns; C) 50 μg/ml Calcofluor white. Means and standard deviations of the germination rate (y-axis) assayed at 6 h were calculated from three replicates.
B. Western blots of proteins isolated from vegetative hyphae of the wild-type strain 70-15 (WT), *mst50* (MF103) and *mps1* (M3H51) treated with 200 μg/ml Calcofluor white for 2 h were probed with the anti-MAPK and anti-TpEY antibodies for the expression and activation levels of Mps1 (46 kDa).

proteins isolated from vegetative hyphae challenged with 200 μg/ml CFW. In comparison with the wild type, the level of Mps1 phosphorylation was significantly reduced in the *mst50* mutant (Fig. 3B). As a control, phosphorylation of Mps1 was not detected in the *mps1* mutant. These results indicate that Mst50 plays a role in the activation of Mps1 in response to cell wall stress in *M. oryzae*.

The sterile alpha-motif (SAM) domain of Mst50 plays a role in responses to cell wall and oxidative stresses

Mst50 has an N-terminal SAM domain and a C-terminal Ras-associated domain (RAD) domain. Strains SD1 (*mst50*/*MST50*$^{\Delta SAM}$) and RD1 (*mst50*/*MST50*$^{\Delta RAD}$) were two transformants of the *mst50* mutant expressing the SAM and RAD domain deletion alleles of *MST50*, respectively (Park *et al*., 2006). Under normal conditions, strains SD1 and RD1 had no defects in conidium germination (Fig. 3A). However, in the presence of 50 μg/ml CFW, only 10% SD1 conidia germinated after incubation for 6 h but conidia of the RD1 strain germinated as efficiently as the wild-type strain (Fig. 3A). These results indicate that deletion of the SAM but not RAD domain affected the function of *MST50* in response to cell wall stress. Interestingly, we found that the *mst50* mutant, like the *mps1* mutant, also had increased sensitivity to H_2O_2 (Supporting Information Fig. S5). Similarly, only the SAM domain of Mst50 was essential for its roles in response to oxidative stress (Supporting Information Fig. S5). Therefore, although both SAM and RAD domains of *MST50* are important for Pmk1 activation and appressorium penetration (Park *et al*., 2006), only the SAM domain plays a critical role in cell wall and oxidative stress responses in *M. oryzae*.

The SAM domain is important for the Mck1-Mst50 interaction

To determine which domain mediated the Mst50-Mck1 interaction, we transformed the Mst50$^{\Delta SAM}$ (SAM-domain deletion) and Mst50$^{\Delta RAD}$ (RAD-domain deletion) prey vectors (Park *et al*., 2006) into the yeast strain YRG-2 with the Mck1 bait vector. Yeast transformants carrying the Mst50$^{\Delta SAM}$ prey and Mck1 bait constructs failed to grow on SD-Leu-Trp-His (SD-His) plates and lacked LacZ activities (Fig. 4A), indicating that Mst50$^{\Delta SAM}$ failed to interact with Mck1 in yeast two-hybrid assays. In contrast, Mst50$^{\Delta RAD}$ still interacted with Mck1 (Fig. 4A). Therefore, the SAM domain but not the RAD domain is important for the Mst50- Mck1 interaction. In contrast, neither Mst50$^{\Delta SAM}$ nor Mst50$^{\Delta RAD}$ interacted with Mkk2 in yeast two-hybrid assays (Fig. 4B), suggesting that the weak interaction between Mst50 and Mkk2 requires both the SAM and RAD domains.

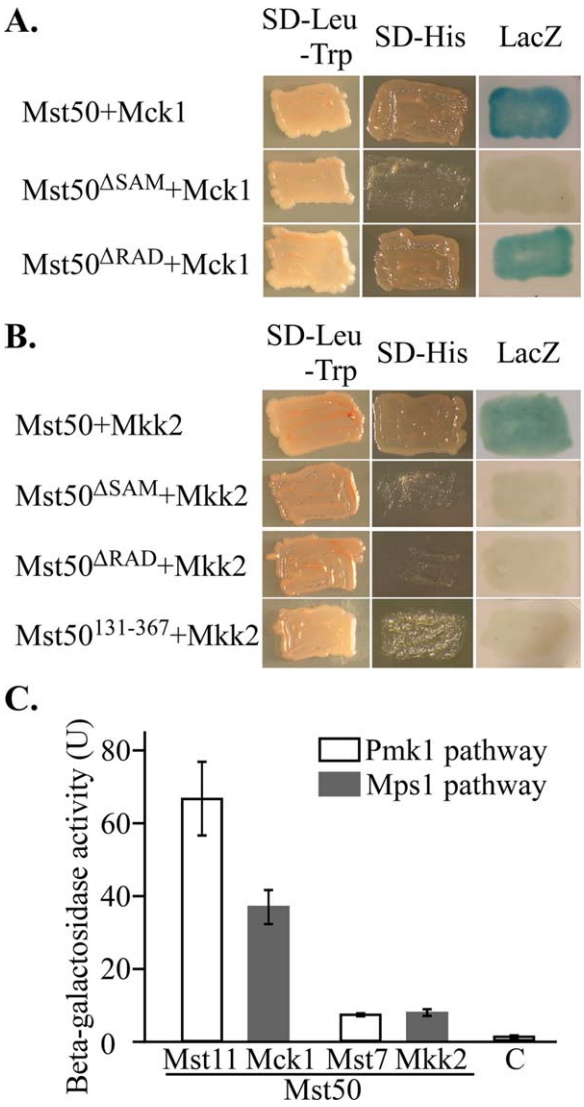

Fig. 4. The roles of SAM and RAD domains in the interaction of Mst50 with Mck1 and Mkk2.
The full-length Mst50, Mst50$^{\Delta SAM}$ (SAM deletion) and Mst50$^{\Delta RAD}$ (RAD deletion) were assayed for their interactions with Mck1 (**A**) and Mkk2 (**B**). Yeast strains expressing marked pairs of bait and prey constructs were assayed for growth on SD-Leu-Trp and SD-Leu-Trp-His (SD-His) plates and β-galactosidase activities. **C.** The β-galactosidase activities in yeast cells expressing marked bait and prey constructs were quantified with O-nitrophenyl-β-D-galactoside (ONPG) as the substrate. Means and standard errors of β -galactosidase activities were calculated from three independent replicates. The Mst50-Pmk1 interaction was used as the negative control (C). The interaction of Mst50 with Mck1 or Mkk2 (grey bars) was weaker than its interaction with Mst11 (the first white bar).
[Colour figure can be viewed at wileyonlinelibrary.com]

Because Mst50 also interacted with Mst11 and Mst7 of the Pmk1 pathway (Park *et al*., 2006), to compare the affinity of Mst50 for Mst11, Mst7, Mck1 and Mkk2, we quantified the β-galactosidase activities in yeast transformants carrying different interacting pairs (Fig. 4C). The yeast

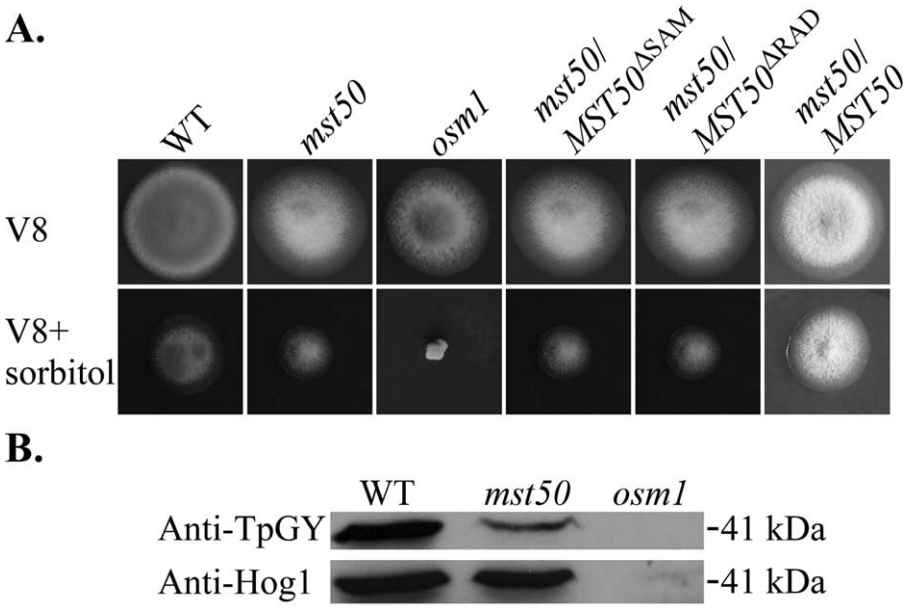

Fig. 5. Assays for sensitivity to osmotic stress and Osm1 phosphorylation in the *mst50* mutant.
A. Five-day-old cultures of the wild-type strain 70-15 (WT), *mst50* mutant MF103, *osm1* mutant JH73, SD1 (*mst50*/*MST50*$^{\Delta SAM}$), RD1 (*mst50*/*MST50*$^{\Delta RAD}$) and *mst50* complementation strain CMF11 (*mst50*/*MST50*) on V8 plates with or without 1 M sorbitol.
B. Western blots of proteins isolated from vegetative hyphae of the wild-type strain 70-15 (WT), *mst50* mutant and *osm1* mutant treated with 1 M sorbitol for 30 min were probed with the anti-TpGY antibody for Osm1 phosphorylation. The expression of Osm1 was detected with the anti-Hog1 antibody.

cells carrying the Mst50-prey and Mst11-bait constructs showed the highest β-galactosidase activity, followed by the Mst50-Mck1 transformant. The interaction of Mst50 with Mkk2 or Mst7 was relatively weak (Fig. 4C).

Deletion of MST50 *also affects Osm1 phosphorylation in response to hyperosmotic stress*

Interestingly, one of the Mst50-interacting proteins (Mip7) is the hybrid histidine kinase Hik1, an osmotic stress sensor unique to filamentous fungi (Motoyama *et al*., 2005). Because Hik1 is important for the activation of Osm1, we assayed the defects of the *mst50* mutant in response to hyperosmotic stress. On regular V8 agar plates, the *mst50* and *osm1* mutants had normal growth rates (Fig. 5A). However, fungal growth was significantly restricted by the presence of 1 M sorbitol in the *osm1* mutant. Under the same conditions, the *mst50* mutant grew faster than the *osm1* mutant but more slowly than the wild type (Fig. 5A), indicating that the *mst50* mutant had increased sensitivity to osmotic stress but was not as hypersensitive as the *osm1* mutant. We also assayed the SD1 (*mst50*/*MST50*$^{\Delta SAM}$) and RD1 (*mst50*/*MST50*$^{\Delta RAD}$) strains for their defects in response to hyperosmotic stress. On V8 agar with 1 M sorbitol, both SD1 and RD1 grew more slowly than the wild-type strain and the *mst50*/*MST50* complemented transformant (Park *et al*., 2006), indicating that both SAM and RAD domains of Mst50 are required for responses to hyperosmotic stress (Fig. 5A).

To determine whether deletion of *MST50* affects the activation of Osm1 MAPK, we assayed its phosphorylation with an anti-TpGY specific antibody. In proteins isolated from vegetative hyphae challenged with 1 M sorbitol for 30 min, Osm1 phosphorylation was significantly reduced in the *mst50* mutant in comparison with the wild type (Fig. 5B). As a negative control, phosphorylation of Osm1 was not detected in the *osm1* mutant. These results further indicate the importance of Mst50 in the activation of the Osm1 MAPK in response to hyperosmotic stress.

Mip11 is involved in regulating the cell wall integrity and Mps1 activation

One of the MIPs is a seven WD40 domain-containing protein, orthologous to Rack1 in mammalian cells (Adams *et al*., 2011) and Asc1 of *S. cerevisiae* (Melamed *et al*., 2010). Co-IP assays were used to verify the Mip11-Mst50 interaction using the anti-Rack1 antibody, which can detect the specific Mip11 band in *M. oryzae* (Supporting Information Fig. S6). In co-IP assays, the anti-FLAG and anti-Rack1 antibodies detected the 52-kDa Mst50 and the 35-kDa Mip11 bands, respectively, from total proteins isolated from the Mst50-3xFLAG transformant and proteins eluted from anti-FLAG M2 beads (Fig. 6A), indicating that Mip11 interacts with Mst50 to form a complex in *M. oryzae*.

To test whether *MIP11* is functional in the budding yeast, its ORF was cloned into the pYES2 vector and transformed into the yeast *asc1* mutant (Melamed *et al*., 2010). The resulting *asc1*/*MIP11* transformant grew as robustly as the *ASC1* strain BY4741 (BY4) on YPGal plates with 100 μg/ml CFW (Fig. 6B). The yeast transformant carrying the empty pYES2 vector could not grow under the same conditions (Fig. 6B), indicating that *MIP11* could complement the defect of the yeast *asc1* mutant in response to cell wall stress.

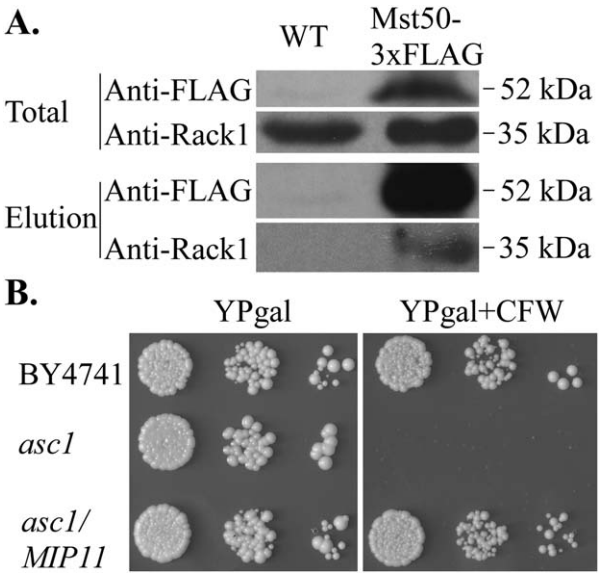

Fig. 6. Assays for the interaction of Mip11 with Mst50 and complementation of the yeast *asc1* mutant.
A. Western blots of total proteins (total) and proteins eluted (elution) from the anti-FLAG M2 beads from the wild-type strain 70-15 (WT) and transformant HZ112 expressing Mst50-3xFLAG were probed with the anti-FLAG and anti-Rack1 antibodies.
B. Expression of *MIP11* suppressed the cell wall integrity defect of the yeast *asc1* mutant. Cultures of yeast strain BY4741 and transformants of the *asc1* mutant carrying empty pYES2 vector (*asc1*) or pYES2-*MIP11* (*asc1*/*MIP11*) were cultured on YPGal plates with or without 100 μg/ml Calcofluor white (CFW) at 30°C for three days.

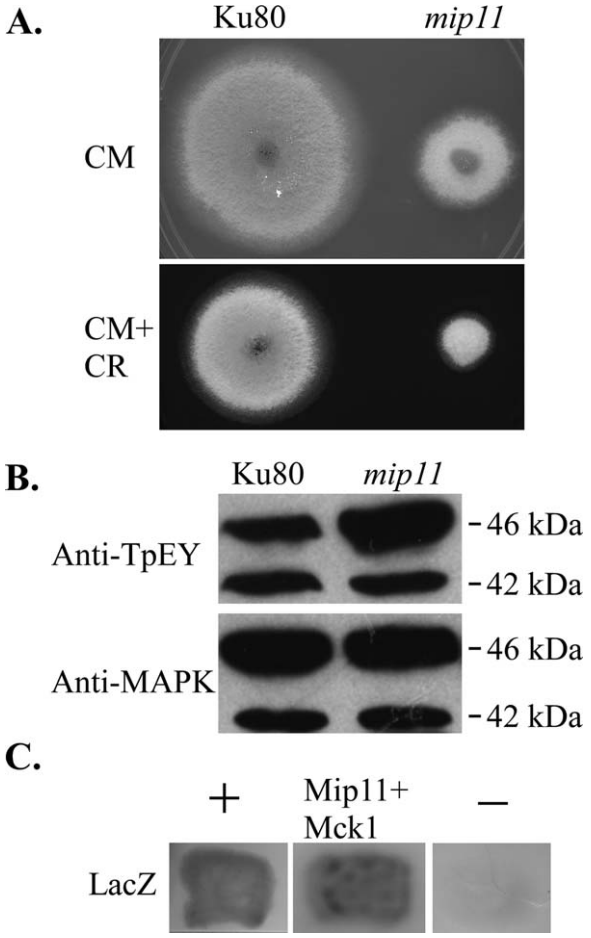

Fig. 7. Defects of the *mip11* mutant in response to cell wall stress.
A. Seven-day-old cultures of the Ku80 strain and the *mip11* mutant Rk26 on CM plates with or without 200 μg/ml Congo red (CR).
B. Western blots of proteins isolated from hyphae of Ku80 and *mip11* mutant Rk26 cultured in CM were probed with the anti-TpEY or anti-MAPK antibody.
C. Yeast transformants expressing the marked bait and prey constructs were assayed for ß-galactosidase activities (LacZ). The Mst50-Mst11 and Mst50-Pmk1 interactions were used as the positive (+) and negative (-) controls respectively.

To determine its function in *M. oryzae*, we generated *mip11* mutants by the gene replacement approach (Supporting Information Fig. S6). In comparison with the wild-type strain, the *mip11* deletion mutant was significantly reduced in growth rate and had increased sensitivity to Congo red (Fig. 7A; Table 3). Because of the apparent cell wall defects of the *mip11* mutant, we assayed the phosphorylation level of Mps1. In comparison with the wild type, the *mip11* mutant was increased in Mps1 phosphorylation (Fig. 7B). In yeast two-hybrid assays, Mip11 directly interacted with Mck1 (Fig. 7C), indicating that Mip11 may affect the phosphorylation of Mps1 via Mck1.

For complementation assays, the Mip11-GFP fusion construct was generated and introduced into the *mip11* mutant. In the resulting transformant RkC18 (Table 1), the cytoplasmic localization of Mip11-GFP fusion proteins was observed in conidia, appressoria and infectious hyphae (Fig. 8). GFP signals were stronger around the nucleus and co-localized with fluorescence signals stained with the ER-Tracker dye (Fig. 8), suggesting the localization of Mip11-GFP to the endoplasmic reticulum at these sites. Transformant RkC18 was recovered in cell wall integrity, growth and conidiation (Table 3). These results indicate that Mip11 is functionally related to cell wall integrity in *M. oryzae*.

The mip11 *deletion mutant is defective in plant infection*

The *mip11* mutant was normal in surface recognition and appressorium formation. After incubation on hydrophobic surfaces for 24 h, over 95% of mutant conidia germinated and a vast majority of the *mip11* germ tubes (81%) formed melanized appressoria (Table 3). These data indicate that *MIP11* is dispensable for conidium germination, surface recognition and appressorium formation.

In infection assays with rice seedlings, typical blast lesions were observed on leaves sprayed with Ku80 or the complementation strain at 7 dpi (Fig. 9A). Under the same conditions, the *mip11* deletion mutant only caused a few small lesions. In infection assays with barley seedlings, the *mip11* mutant also was significantly reduced in virulence

Table 3. Phenotypic characterization of the *mip11* mutant in *M. oryzae*.

Strain	Growth rate (mm/day)[a]	Conidiation (10^5 spores/plate)[a]	Conidium germination (%)[b]	Appressorium formation (%)[b]	Inhibition (%)[c]	
					Congo red	Sorbitol
Ku80	2.9 ± 0.1	87.5 ± 12.6	97.7 ± 1.2	99.0 ± 1.1	21.8 ± 2.0	34.8 ± 1.7
mip11	1.6 ± 0.1	1.7 ± 1.5	94.0 ± 3.6	80.7 ± 3.6	43.0 ± 3.8	35.2 ± 3.3
mip11/MIP11	2.5 ± 0.1	16.3 ± 2.0	94.0 ± 2.0	96.1 ± 2.4	27.5 ± 0.9	N/A[d]

a. The growth rate and conidiation was measured on CM cultures. Means and standard deviations were calculated with results from three replicates.
b. Percentage of conidium germination and appressorium formation by 24 h. Means and standard deviations were calculated from three independent repeats (at least 100 conidia were counted in each repeat).
c. The inhibition extent (%) = [(the diameter of regular CM cultures − the diameter of cultures on CM with different chemical)/the diameter of regular CM cultures]×100. Two hundred μg/ml Congo red and 1 M sorbitol were used in the stress tests, respectively. Data from three replicates were analyzed with the two sample t-test.
d. Not assayed.

(Fig. 9B). Five days after inoculation, both Ku80 and the complementation strain formed numerous lesions with green islands on barley leaves. In contrast, the *mip11* mutant only caused a few limited necrotic spots. In rice sheath penetration assays, strain Ku80 formed abundant invasive hyphae in penetrated epidermal cells and spread to neighboring plant cells by 48 h post inoculation (hpi) (Fig. 9C). Under the same conditions, the *mip11* mutant had only limited growth of invasive hyphae in the first penetrated plant cells. Even after prolonged incubation, extensive growth of invasive hyphae was only observed in plant tissues inoculated with Ku80 but not the *mip11* mutant. These results indicate that although it is dispensable for appressorium formation, *MIP11* plays an important role in invasive growth and disease development.

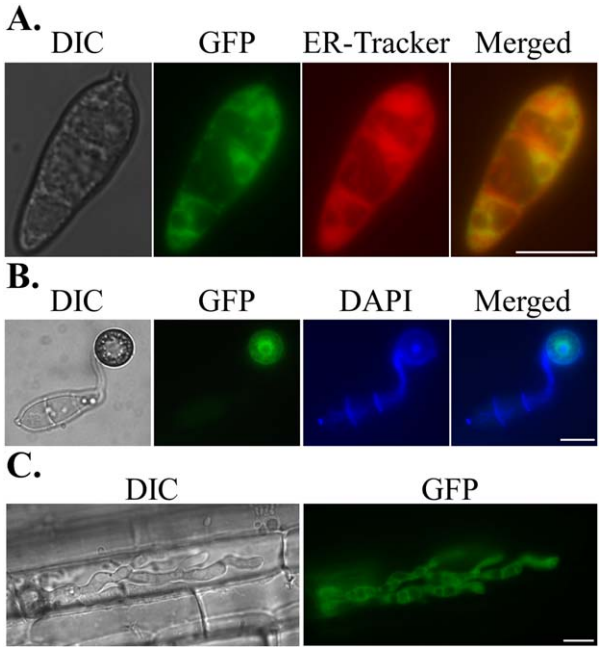

Fig. 8. Subcellular localization of Mip11-GFP.
A. Conidia of the Mip11-GFP transformant (RkC18) were examined by DIC (differential interference contrast) and epifluorescence microscopy after staining with the ER-Tracker dye Blue-White DPX.
B. Appressoria of the Mip11-GFP transformant (RkC18) were examined by DIC and epifluorescence microscopy. Appressoria were stained with 4′, 6-diamidino-2-phenylindole (DAPI) to visualize nuclei.
C. Invasive hyphae of transformant RkC18 developed in penetrated rice epidermal cells were examined for the expression and localization of Mip11-GFP under DIC and epifluorescence microscopy. Bar = 10 μm. [Colour figure can be viewed at wileyonlinelibrary.com]

Two Mst50-interacting proteins, Mip13 and Mip14, may be essential for growth in M. oryzae

Two of the MIPs confirmed by co-IP assays were Mip13 and Mip14 (Fig. 1). *MIP13* is orthologous to *SUM2*, which encodes a G2/M phase checkpoint control protein that is important for cell cycle control in *Schizosaccharomyces pombe* (Reynolds and Ohkura, 2003). In *M. oryzae*, one round of special mitosis in the germ tube is required for appressorium formation, in which the nuclear division is spatially uncoupled from the site of cytokinesis and septum formation (Saunders *et al.*, 2010a). In contrast, the *pmk1* mutant that is defective in appressorium formation undergoes coupled mitosis and cytokinesis in germ tubes (Saunders *et al.*, 2010a,b). It is possible that the interaction between Mip13 and Mst50 plays a role in coordinating cell cycle and regulation of appressorium formation by the Pmk1 pathway. Unfortunately, we failed to identify putative *mip13* deletion mutants after screening over 100 transformants in repeated transformations, suggesting that it may be an essential gene in *M. oryzae*.

The *MIP14* gene is orthologous to *YPP1*. In the budding yeast, *YPP1* is an essential gene that encodes a cargo-transport protein involved in endocytosis. Its interaction with the phosphatidylinositol-4-kinase Stt4 is required for the assembly of the Stt4 complex at the cytoplasm membrane (Zhai *et al.*, 2008). In repeated attempts, we failed to identify *mip14* deletion mutants. Therefore, the

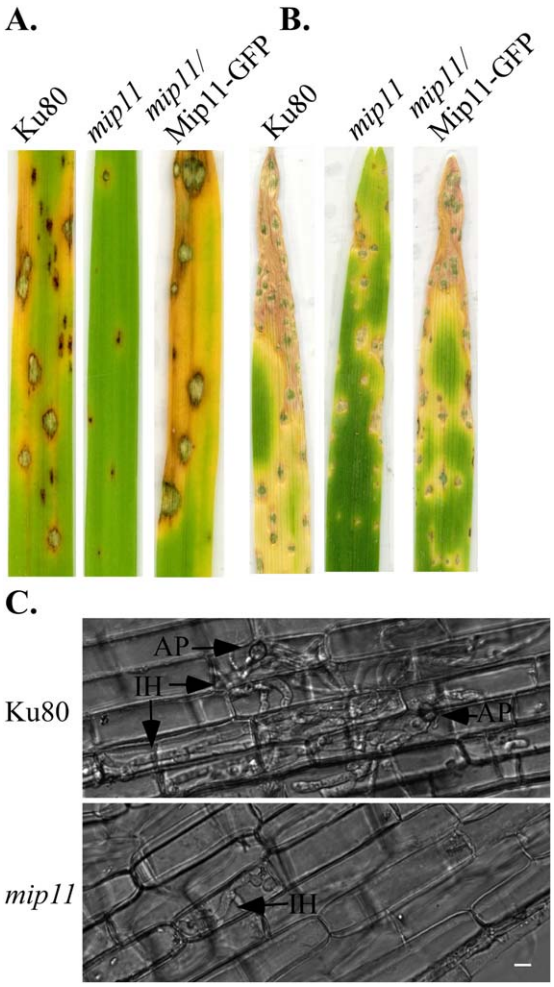

Fig. 9. Infection assays with the *mip11* mutant.
A. Seedlings of rice cultivar CO-39 were sprayed with conidia of Ku80, the *mip11* mutants Rk26, and the complementation strain RkC18 (*mip11*/Mip11-GFP).
B. Ten-day-old barley seedlings were sprayed with conidia of strains Ku80, *mip11* and *mip11*/Mip11-GFP. Photos were taken five days post inoculation.
C. Penetration assays with the *mip11* mutant. Rice leaf sheaths inoculated with conidia of Ku80 and the *mip11* mutant Rk26 were examined 48 hpi. AP, appressorium; IH, invasive hyphae.
Bar = 10 μm. [Colour figure can be viewed at wileyonlinelibrary.com]

biochemical function of *MIP14* and the role of its interaction with Mst50 remain unclear in *M. oryzae*.

Deletion of MIP17*, encoding a novel Mst50-interacting protein, has no obvious phenotype*

We also selected Mip17 that has no distinct orthologues in *S. cerevisiae* for functional characterization. *MIP17* encodes a hypothetical protein that is conserved only in some ascomycete pathogens, including *Gaeumannomyces graminis* and *Verticillium dahliae*. Two *mip17* deletion mutants were identified and confirmed by Southern blot analysis (Supporting Information Fig. S7; Table S2). The mutant had normal growth rate and colony morphology. The mutant had no obvious defects in appressorium formation, virulence and stress responses (Supporting Information Fig. S7), indicating that although it interacts with Mst50, Mip17 plays no or only a minor role in the activation of the Pmk1 pathway.

Discussion

The adaptor and scaffold proteins in signal transduction pathways link different signal transduction components together to form large signaling complexes and facilitate signal transduction (Flynn, 2001). Mst50, a SAM domain-containing protein, is originally identified as an adaptor protein for the Pmk1 pathway in *M. oryzae* (Park *et al*., 2006). The SAM domain has been identified in various proteins in diverse eukaryotes and is widely involved in many biological processes by forming homo- and hetero-oligomers with SAM domain-containing proteins or other partners (Kim and Bowie, 2003). In this study, Mst50-interacting proteins were identified by the affinity purification approach. Two of them, Mst11 and Mst7 are known to physically interact with Mst50 and functionally related to the Pmk1 MAPK pathway (Zhao *et al*., 2005; Park *et al*., 2006). Six other MIPs were confirmed by co-IP assays for their interactions with Mst50, including Chm1 that may be functionally related to the Pmk1 pathway. Although it is dispensable for appressorium formation, it remains possible that Chm1 may have overlapping functions with Ste20 in the activation of the Pmk1 pathway because the *chm1 ste20* mutant appeared to be inviable (Li *et al*., 2012). Chm1 interacts with MgRac1 and plays a regulatory role in appressorium penetration and plant infection (Chen *et al*., 2008). Similar to Chm1, the Cdc42 orthologue, a putative component of the Pmk1 pathway, is also dispensable for appressorium formation but is important for appressorium morphogenesis and function in *M. oryzae* (Park *et al*., 2006; Zheng *et al*., 2009; Dagdas *et al*., 2012). Mst12, one of the downstream targets of Pmk1, is important for proper cytoskeleton reorganization at late stages of appressorium development (Dagdas *et al*., 2012). Therefore, the Mst50-Chm1 interaction may be not important for appressorium formation but plays a role in regulating cytoskeleton organization, appressorium morphogenesis and penetration in *M. oryzae*. In *U. maydis*, two PAK kinases, Smu1 (Mst20 homolog) and Cla4, have shown differential effects on mating and pathogenesis that are regulated by the Kpp4-Kpp6 MAPK pathway (Banuett *et al*., 2008; Garcia-Pedrajas *et al*., 2008).

Interestingly, Mst50 also interacted with Mck1 and Mkk2, the MEKK and MEK of the Mps1 MAPK pathway in *M. oryzae*. In *S. cerevisiae*, Bck1 is not one of the Ste50-interacting proteins identified by affinity purification (Cherry

et al., 2012). However, the Ste50 orthologue in *Neurospora crassa* functions as the adaptor for the MAK-2 MAPK (Jonkers *et al.*, 2014) but it also forms a protein complex with Mak1 (yeast Slt2) (Dettmann *et al.*, 2014). In *M. oryzae*, the involvement of Mst50 in the Mps1 pathway may be primarily mediated by Mck1 because of its stronger interaction with Mck1 than with Mkk2. However, the affinity of Mst50 for Mst11 was stronger than that for Mck1, which is consistent with the fact that Mst50 plays a more critical role in the Pmk1 pathway than in the Mps1 pathway. Phenotypically, the *mst50* mutant is similar to the *pmk1* mutant in appressorium formation but only partially similar to the *mps1* mutant in cell wall integrity defects. In the TEY assays, the phosphorylation level of Mps1 is partially reduced in the *mst50* mutant, whereas the activation of Pmk1 is completely blocked. One likely explanation for the difference in the importance of Mst50 in the Pmk1 and Mps1 pathways is that Mst11 and Mst7 do not interact with each other directly and their associations with Mst50 is required for the signal transduction from Mst11 to Mst7 (Zhao *et al.*, 2005). In contrast, Mck1 and Mkk2 directly interacted with each other in yeast two-hybrid assays (Fig. 2). It is likely that their interactions with Mst50 are important but not essential for Mps1 activation in *M. oryzae*.

The two domains of Mst50 played different roles in the response to stresses. Deletion of the SAM domain resulted in transformants that were hypersensitive to cell wall stress and H_2O_2. In yeast two-hybrid assays, the SAM domain was required for the interaction of Mst50 with Mck1, which is consistent with the essential role of the SAM domain in stress responses. Similarly, the SAM domain is required for appressorium formation, plant infection and the interaction with Mst11 (Park *et al.*, 2006). In contrast, the RAD domain was not important for responses to cell wall or H_2O_2 stress, which was in agreement with the dispensable role of the RAD domain in the Mst50-Mck1 interaction. In *S. cerevisiae*, both SAM and RAD domains are critical for Ste50 functions (Ramezani-Rad, 2003). However, in the human pathogen *C. neoformans*, the SAM domain rather than the RAD domain plays a major role in Ste50 functions during monokaryotic fruiting and sexual reproduction (Fu *et al.*, 2011). Taken together, the SAM domain is required for conserved Ste50 functions but the function of the RAD domain may vary among different fungi.

Furthermore, we found that Mst50 also is involved in the Osm1 pathway in *M. oryzae*. The *mst50* mutant was more sensitive to 1 M sorbitol and the deletion of *MST50* resulted in a significant reduction of Osm1 phosphorylation, indicating that Mst50 is required for proper Osm1 activation under osmotic stress. Unlike its role in the Mps1 pathway, both SAM and RAD domains of Mst50 are required for its function in osmotic stress response. Our data showed that Mst50 physically associates with Hik1 but the exact role of Mst50 in the Osm1 pathway remains to be characterized. In *N. crassa*, Ste50 could form a complex with several members of the osmoregulation pathway, including Os-2, Cut-1 and Asl-1 (Dettmann *et al.*, 2014; Jonkers *et al.*, 2014). In *M. oryzae*, orthologues of these *N. crassa* proteins were not among the MIPs identified by affinity purification. Interestingly, the *mst50* and *mps1* mutants but not the *osm1* mutant were hypersensitive to H_2O_2 stress and the SAM domain of Mst50 played a major role in H_2O_2 stress response, which is consistent with a previous study showing that the phosphorylation of Osm1 was not induced by H_2O_2 stimulation (Motoyama *et al.*, 2008). Although Hog1 is the MAPK regulating responses to oxidative stress in many fungi, the Mps1 pathway is involved in reactive oxygen species (ROS) responses in some fungi, such as *Aspergills fumigatus* (Jain *et al.*, 2011). In *M. oryzae*, the role of Mst50 in response to oxidative stress is likely mediated via the Mps1 pathway.

Mip11, a seven WD40 domain-containing protein, is one of the Mst50-interacting proteins identified in this study. The association between Mip11 and Mst50 was confirmed by co-IP assays. In yeast two-hybrid assays, Mip11 interacted directly with Mck1 of the Mps1 pathway. The *mip11* mutant was hypersensitive to cell wall stress, which is similar to mutants deleted of its orthologues in *S. cerevisiae* and *U. maydis* (Wang *et al.*, 2011; Rachfall *et al.*, 2013). However, the level of Mps1 phosphorylation in the *mip11* mutant was higher than that in the wild-type strain. It is possible that defects of the *mip11* mutant in cell wall integrity increased the phosphorylation of Mps1 but the activation of Mps1 MAPK alone was not sufficient to repair its cell wall defects, likely due to down-regulation of genes involved in cell wall synthesis. In *S. cerevisiae*, the *asc1* mutant also had cell wall defects although it was increased in the activation of the cell wall integrity Slt2 MAPK pathway (Rachfall *et al.*, 2013). Many genes related to cell wall biogenesis were down-regulated in the *asc1* mutant (Rachfall *et al.*, 2013), suggesting the involvement of others factors regulating their expression in yeast. Nevertheless, subcellular compartmentalization of MAPK modules and their dynamic shuffle between the nucleus and cytoplasm are important for optimal MAPK functions (Chen *et al.*, 2010). It is possible that the interaction of Mck1 with Mip11 is important for the dynamic localization of components of the Mps1 cascade and the absence of Mip11 may affect their subcellular localization or nucleo-cytoplasmic shuffle although Mps1 is over-activated. The *mip11* mutant was reduced in virulence, likely resulting from its defects in cell wall integrity that is known to be important for plant penetration and invasive growth (Xu *et al.*, 1998). In *U. maydis* and *V. dahliae*, the *rack1* mutants also were reduced in virulence (Wang *et al.*, 2011; Yuan *et al.*, 2017). Although it has not been reported in fungi, the scaffolding roles of Rack1 proteins in MAPK pathways are well documented (Cheng *et al.*, 2015; Li and Xie, 2015). In *N. crassa*, HAM-

5, another seven WD40 domain-containing protein, functions as a scaffold protein for the MAK-2 MAP kinase complex (Jonkers *et al*., 2014), indicating that this class of proteins may be important for MAPK signaling in filamentous fungi.

Overall, our results showed that Mst50 is functionally related to all three MAPK pathways in *M. oryzae*, which is similar to the involvement of Ste50 in the Fus3 mating, Kss1 invasive/filamentous growth and Sho1-dependent Hog1 MAPK pathways in *S. cerevisiae* (Jansen *et al*., 2001; Ramezani-Rad, 2003; Kwan *et al*., 2006; Truckses *et al*., 2006). In *N. crassa*, Ste50 not only appears to be related to the MAK-2 MAPK but also forms protein complexes with Mak1 (yeast Slt2) and multiple components of the Hog1 MAPK pathway (Dettmann *et al*., 2014; Jonkers *et al*., 2014). It is likely that Ste50 orthologues have conserved functions in mediating protein-protein interactions and multiple signaling pathways in many filamentous fungi. However, the importance and functions of Mst50 in each pathway are different in *M. oryzae*. As an adaptor protein, Mst50 plays an essential role in the activation of Pmk1 MAPK for appressorium formation in *M. oryzae* (Park *et al*., 2006) but the *mst50* mutant was only reduced in the Mps1 and Osm1 phosphorylation. Although it is involved, Mst50 is not essential for the cell wall integrity and osmoregulation pathways. Mip11 may facilitate the interaction of Mst50 with Mck1 but the roles of Mst50-Mip11 and Mip11-Mck1 associations in the cell wall integrity pathway need to be further characterized. The interaction of Mst50 with Hik1 and the functional relationship between Mst50 and the Osm1 pathway also needs to be further characterized. Furthermore, several putative Mst50-interacting proteins identified in this study are conserved in filamentous ascomycetes but lack distinct orthologues in the budding yeast, such as Mip12 and Mip17. Although its function is not clear, *MIP12* encodes a putative Ser/Thr protein phosphatase that is expressed during appressorium formation and biotrophic invasive growth *in planta* (Kour *et al*., 2012). It is possible that the interactions of Mst50 with Mip12, Rho1 and other Mst50-interacting proteins are important for proper responses to various external stress or signals and crosstalk among these different signaling pathways.

Experimental procedures

Strains and growth conditions

All the *M. oryzae* wild-type and mutant strains (Table 1) were cultured on oatmeal agar (OA), complete medium (CM), or V8 agar as described previously (Ding *et al*., 2010). Protoplast preparation and transformation were performed as described (Zhou *et al*., 2011). Transformants were selected on medium with 250 μg/ml hygromycin B (Calbiochem), 300 μg/ml zeocin (Invitrogen) or 400 μg/ml geneticin (MP Biochemicals). The growth rate of different strains was measured on CM plates and conidiation was measured with OA cultures as described (Liu *et al*., 2011). Growth rate or conidium germination in the presence of 200 μg/ml Congo red, 50 μg/ml CFW, 5 mM H_2O_2, or 1 M sorbitol was assayed as described (Park *et al*., 2006; Guo *et al*., 2011; Yin *et al*., 2015).

Affinity purification and MS analysis

The Mst50-3xFLAG fusion was constructed via the yeast gap repair approach (Bourett *et al*., 2002). The PCR products amplified with primers 50FG/F and 50FG/R from genomic DNA were co-transformed with *Xho*I-digested pHZ126 or *Xho*I-digested pFL5 into yeast. The resulting constructs pHZ112 and pHZ115 were transformed into the wild-type strain 70-15 and the *mst50* mutant MF103. The expression of Mst50-3xFLAG construct was confirmed by western blot analysis with an anti-FLAG antibody (Sigma-Aldrich). For affinity purification, total proteins were isolated from transformant HZ112 and incubated as described (Ding *et al*., 2010; Zhou *et al*., 2012) with anti-FLAG M2 affinity resins (Sigma-Aldrich). After washing three times each with 500 μl of lysis buffer, 50 mM TMAB (trimethylammonium bicarbonate, Fluka), and ddH_2O, Mst50-interacting proteins were eluted with 0.1% Rapigest (Waters Corporation) and analysed by Nanoflow liquid chromatography tandem mass spectrometry (nLC-MS/MS) after digestion with trypsin (Ding *et al*., 2010; Zhou *et al*., 2012). The resulting MS data were used to search against the National Center for Biotechnology Information (NCBI) nonredundant *M. oryzae* protein database to identify Mst50-interacting proteins as described (Zhou *et al*., 2012).

Co-immunoprecipitation assays

To generate the Mck1-3xFLAG construct, PCR products amplified with primer pair MIP4/F-R were co-transformed with the *Xho*I-digested pHZ126 (Zhou *et al*., 2011) into yeast strain XK1-25 as described (Bruno *et al*., 2004). The resulting plasmid pYE8 was transformed into *M. oryzae* strain 70-15. Transformants containing construct pYE8 were identified by PCR and the expression of Mck1-3xFLAG fusion was confirmed by western blot analysis. Total proteins isolated from the resulting Mck1-3xFLAG transformant were incubated with anti-FLAG M2 affinity resins (Sigma-Aldrich) at 4°C overnight. Proteins bound to anti-FLAG beads were eluted and used for western blot analysis. Gel conditions, transfer and detection with the anti-FLAG (Sigma-Aldrich), anti-actin (Sigma-Aldrich), or anti-Mst50 antibodies were performed as described (Ding *et al*., 2010; Liu *et al*., 2011). The rabbit anti-Mst50 antibody was generated with the synthetic oligopeptide (AEASP-TESDPPSNEC) of Mst50 by GenScript Corp (Piscataway, NJ, USA). The same approach was used for co-IP assays with other Mst50-interacting proteins.

Generation of the MIP11 *and other* MIP *gene knockout constructs and mutants*

The double-joint PCR approach (Yu *et al*., 2004) was used to generate the *MIP11* gene replacement constructs (Supporting Information Fig. S6). The approximately 1-kb upstream and 1-kb downstream flanking sequences of *MIP11* were amplified with primer pairs MIP11/1F-2R and MIP11/3F-4R (Supporting

Information Table S1), respectively, and overlapped with the *hph* cassette. The overlapping PCR products were transformed into protoplasts of strain Ku80 (Villalba *et al.*, 2008). Putative *MIP11* gene replacement mutants were identified by PCR and confirmed by Southern blot analysis. Similar approaches were used to generate gene replacement construct and knockout mutants for the other *MIP* genes.

For complementation assays, the wild-type allele of *MIP11* (without the stop codon) amplified with primer pairs MIP11GFP/F-R was cloned into plasmid pFL2 by the yeast GAP repair approach as described (Bruno *et al.*, 2004; Zhou *et al.*, 2011). The *MIP11*-GFP fusion rescued from resulting Trp^+ yeast transformants was verified by sequencing analysis and transformed into protoplasts of the *mip11* mutant Rk26. The resulting transformants were examined for GFP signals and stained with the ER-Tracker Blue-White DPX (Molecular Probes) or 4′,6-diamidino-2-phenylindole (DAPI) (Sigma-Aldrich) as described (Yi *et al.*, 2009; Zhou *et al.*, 2012).

Appressorium formation and plant infection assays

For appressorium formation assays, conidia were collected from ten-day-old OA cultures and re-suspended to $5x10^4$ conidia/ml in sterile distilled water. A drop of 20 μl of conidium suspension was placed on cover slips and examined for conidium germination and appressorium formation as described (Liu *et al.*, 2011). For plant infection assays, freshly harvested conidia were resuspended to a concentration of $5x10^4$ conidia/ml in 0.25% gelatin as described (Wang *et al.*, 2015). Seedlings of two-week-old rice cultivar CO-39 or ten-day-old barley cultivar Golden Promise were used for infection assays (Wang *et al.*, 2015). Plant inoculation, incubation and lesion examination were conducted as described (Liu *et al.*, 2011). Penetration assays with rice leaf sheaths were performed as described (Li *et al.*, 2011; Zhou *et al.*, 2012).

Yeast two-hybrid assays

For assaying protein-protein interactions with the Hybrid-Zap2.1 yeast two-hybrid system (Stratagene), the ORF of *MCK1* was amplified with primers MCK/BDF-R and cloned into pBD-GAL4-2.1 as the bait construct. The prey constructs of *MKK2* and *MIP11* were generated with the prey vector AD-GAL4-2.1. The bait or prey constructs of *MST50*, $MST50^{\Delta SAM}$ (SAM domain deletion), and $MST50^{\Delta RAD}$ (RAD domain deletion) were generated in previous studies (Zhao *et al.*, 2005; Park *et al.*, 2006; Zhou *et al.*, 2012). All the bait and prey constructs were co-transformed in pairs into yeast strain YRG-2 with the alkali-cation yeast transformation kit (MP Biomedicals). The resulting yeast cells that grew on SD-Leu-Trp were further assayed for growth on SD-Leu-Trp-His (SD-His) medium and the expression of the LacZ reporter gene with X-Gal (Zhao *et al.*, 2005). O-nitrophenyl-β-D-galactoside (ONPG) was used as the substrate to assay β-galactosidase activities quantitatively as described (Lai *et al.*, 2011). Briefly, we used OD_{420} to measure the concentration of o-nitrophenol, a yellow chromogenic compound from ONPG hydrolyzed by β-galactosidase. We used OD_{600} to measure the concentration of yeast cells used in the assay. One unit of the β-galactosidase activity was defined as one tenth of OD_{420}/OD_{600}. Yeast transformants YGP5 and YGP10 generated in a previous study (Zhao *et al.*, 2005) were used as the positive and negative controls respectively.

Assays for Pmk1, Mps1 and Osm1 phosphorylation

Total proteins were isolated from vegetative hyphae with protein extraction buffer containing protease inhibitor cocktail (Sigma-Aldrich) and phosphatase inhibitor cocktail 2 (Sigma-Aldrich) as described (Ding *et al.*, 2010). For stress conditions, hyphae isolated from two-day-old 5xYEG cultures were further incubated in 5xYEG medium with 200 μg/ml CFW or 1 M sorbitol for 30 min. For western blot analysis, proteins were separated on 10% SDS-PAGE gels and transferred onto nitrocellulose membranes as described (Wang *et al.*, 2015). The expression and activation of Mps1 and Pmk1 MAP kinases were detected with the anti-p44/42 and the phospho-p44/42 MAP kinase antibody kits (Cell Signaling Technology). The expression and activation of Osm1 were detected with anti-Hog1 antibody (Santa Cruz Biotechnology) and the phospho-p38 MAP kinase antibody kit (Cell Signaling Technology) respectively. The SuperSignal West Femto chemiluminescent substrate (Thermo Scientific) was used for the antigen-antibody detection.

Yeast complementation analysis

The *MIP11* ORF was amplified with primers MIP11/YCF-YCR (Supporting Information Table S1) from the cDNA of Guy11 and cloned into the yeast complementation vector pYES2 (Invitrogen). Competent cells of the *asc1* mutant (Melamed *et al.*, 2010) (Open Biosystems, AL) were prepared and transformed with pYES2-*MIP11* or the empty pYES2 vector with the alkali-cation yeast transformation kit (MP Biomedicals, OH). $Ura3^+$ transformants were isolated and assayed for the growth on YPGal plates with or without 100 μg/ml CFW. Yeast strain BY4741 (*MATa his3 leu2 met15 ura3*) used to generate the *asc1* mutant was used as the control.

Acknowledgements

We thank Dr. Steve Goodwin at Purdue University for critical reading of this manuscript. This work was supported by grants from the USDA Integrated Research Program (#2007-35319-102681) and from USDA-NIFA (2012-67013-19381). GL was partially supported by a CSC fellowship (#2008630021). The authors have no conflict of interest.

References

Adams, D.R., Ron, D., and Kiely, P.A. (2011) RACK1, A multifaceted scaffolding protein: Structure and function. *Cell Commun Signal* **9:** 22.

Banuett, F., Quintanilla, R.H., Jr., and Reynaga-Pena, C.G. (2008) The machinery for cell polarity, cell morphogenesis, and the cytoskeleton in the Basidiomycete fungus *Ustilago maydis*-a survey of the genome sequence. *Fungal Genet Biol* **45:** S3–S14.

Bourett, T.M., Sweigard, J.A., Czymmek, K.J., Carroll, A., and Howard, R.J. (2002) Reef coral fluorescent proteins for

visualizing fungal pathogens. *Fungal Genet Biol* **37:** 211–220.

Bruno, K.S., Tenjo, F., Li, L., Hamer, J.E., and Xu, J.R. (2004) Cellular localization and role of kinase activity of PMK1 in *Magnaporthe grisea*. *Eukaryot Cell* **3:** 1525–1532.

Chao, C., and Ellingboe, Y. (1991) Selection for mating competence in *Magnaporthe grisea* pathogenic to rice. *Can J Bot* **69:** 5.

Chen, J.S., Zheng, W., Zheng, S.Q., Zhang, D.M., Sang, W.J., Chen, X., *et al*. (2008) Rac1 is required for pathogenicity and Chm1-dependent conidiogenesis in rice fungal pathogen *Magnaporthe grisea*. *Plos Pathog* **4:** e1000202.

Chen, R.E., Patterson, J.C., Goupil, L.S., and Thorner, J. (2010) Dynamic localization of Fus3 mitogen-activated protein kinase is necessary to evoke appropriate responses and avoid cytotoxic effects. *Mol Cel Biol* **30:** 4293–4307.

Chen, X.L., Shi, T., Yang, J., Shi, W., Gao, X., Chen, D., *et al*. (2014) N-glycosylation of effector proteins by an alpha-1,3-mannosyltransferase is required for the rice blast fungus to evade host innate immunity. *Plant Cell* **26:** 1306–1376.

Cheng, Z., Li, J.F., Niu, Y., Zhang, X.C., Woody, O.Z., Xiong, Y., *et al*. (2015) Pathogen-secreted proteases activate a novel plant immune pathway. *Nature* **521:** 213–216.

Cherry, J.M., Hong, E.L., Amundsen, C., Balakrishnan, R., Binkley, G., Chan, E.T., *et al*. (2012) Saccharomyces Genome Database: the genomics resource of budding yeast. *Nucleic Acids Res* **40:** D700–D705.

Choi, W., and Dean, R.A. (1997) The adenylate cyclase gene MAC1 of *Magnaporthe grisea* controls appressorium formation and other aspects of growth and development. *Plant Cell* **9:** 1973–1983.

Dagdas, Y.F., Yoshino, K., Dagdas, G., Ryder, L.S., Bielska, E., Steinberg, G., and Talbot, N.J. (2012) Septin-mediated plant cell invasion by the rice blast fungus, *Magnaporthe oryzae*. *Science* **336:** 1590–1595.

Dean, R.A., Talbot, N.J., Ebbole, D.J., Farman, M.L., Mitchell, T.K., Orbach, M.J., *et al*. (2005) The genome sequence of the rice blast fungus *Magnaporthe grisea*. *Nature* **434:** 980–986.

Dettmann, A., Heilig, Y., Valerius, O., Ludwig, S., and Seiler, S. (2014) Fungal communication requires the MAK-2 pathway elements STE-20 and RAS-2, the NRC-1 adapter STE-50 and the MAP kinase scaffold HAM-5. *PLoS Genet* **10:** e1004762.

Ding, S.L., Liu, W., Iliuk, A., Ribot, C., Vallet, J., Tao, A., *et al*. (2010) The tig1 histone deacetylase complex regulates infectious growth in the rice blast fungus *Magnaporthe oryzae*. *Plant Cell* **22:** 2495–2508.

Dixon, K.P., Xu, J.R., Smirnoff, N., and Talbot, N.J. (1999) Independent signaling pathways regulate cellular turgor during hyperosmotic stress and appressorium-mediated plant infection by *Magnaporthe grisea*. *Plant Cell* **11:** 2045–2058.

Flynn, D.C. (2001) Adaptor proteins. *Oncogene* **20:** 6270–6272.

Fu, J., Mares, C., Lizcano, A., Liu, Y., and Wickes, B.L. (2011) Insertional mutagenesis combined with an inducible filamentation phenotype reveals a conserved STE50 homologue in *Cryptococcus neoformans* that is required for monokaryotic fruiting and sexual reproduction. *Mol Microbiol* **79:** 990–1007.

Garcia-Pedrajas, M.D., Nadal, M., Bolker, M., Gold, S.E., and Perlin, M.H. (2008) Sending mixed signals: redundancy vs. uniqueness of signaling components in the plant pathogen, *Ustilago maydis*. *Fungal Genet Biol* **45(Suppl.1):** S22–S30.

Giraldo, M.C., Dagdas, Y.F., Gupta, Y.K., Mentlak, T.A., Yi, M., Martinez-Rocha, A.L., *et al*. (2013) Two distinct secretion systems facilitate tissue invasion by the rice blast fungus *Magnaporthe oryzae*. *Nat Commun* **4:** 1996.

Guo, M., Chen, Y., Du, Y., Dong, Y., Guo, W., Zhai, S., *et al*. (2011) The bZIP transcription factor MoAP1 mediates the oxidative stress response and is critical for pathogenicity of the rice blast fungus *Magnaporthe oryzae*. *PLoS Pathog* **7:** e1001302.

Howard, R.J., Ferrari, M.A., Roach, D.H., and Money, N.P. (1991) Penetration of hard substrates by a fungus employing enormous turgor pressures. *Proc Natl Acad Sci U S A* **88:** 11281–11284.

Jain, R., Valiante, V., Remme, N., Docimo, T., Heinekamp, T., Hertweck, C., *et al*. (2011) The MAP kinase MpkA controls cell wall integrity, oxidative stress response, gliotoxin production and iron adaptation in *Aspergillus fumigatus*. *Mol Microbiol* **82:** 39–53.

Jansen, G., Buhring, F., Hollenberg, C.P., and Rad, M.R. (2001) Mutations in the SAM domain of STE50 differentially influence the MAPH-mediated pathways for mating, filamentous growth and osmotolerance in *Saccharomyces cerevisiae*. *Mol Genet Genomics* **265:** 102–117.

Jeon, J., Goh, J., Yoo, S., Chi, M.H., Choi, J., Rho, H.S., *et al*. (2008) A putative MAP kinase kinase kinase, MCK1, is required for cell wall integrity and pathogenicity of the rice blast fungus, *Magnaporthe oryzae*. *Mol Plant Microbe Interact* **21:** 525–534.

Jonkers, W., Leeder, A.C., Ansong, C., Wang, Y., Yang, F., Starr, T.L., *et al*. (2014) HAM-5 functions as a MAP kinase scaffold during cell fusion in *Neurospora crassa*. *PLoS Genet* **10:** e1004783.

Kankanala, P., Czymmek, K., and Valent, B. (2007) Roles for rice membrane dynamics and plasmodesmata during biotrophic invasion by the blast fungus. *Plant Cell* **19:** 706–724.

Kim, C.A., and Bowie, J.U. (2003) SAM domains: uniform structure, diversity of function. *Trends Biochem Sci* **28:** 625–628.

Kour, A., Greer, K., Valent, B., Orbach, M.J., and Soderlund, C. (2012) MGOS: development of a community annotation database for *Magnaporthe oryzae*. *Mol Plant Microbe Interact* **25:** 271–278.

Kramer, B., Thines, E., and Foster, A.J. (2009) MAP kinase signalling pathway components and targets conserved between the distantly related plant pathogenic fungi *Mycosphaerella graminicola* and *Magnaporthe grisea*. *Fungal Genet Biol* **46:** 667–681.

Kwan, J.J., Warner, N., Maini, J., Tung, K.W.C., Zakaria, H., Pawson, T., and Donaldson, L.W. (2006) *Saccharomyces cerevisiae* Ste50 binds the MAPKKK Ste11 through a head-to-tail SAM domain interaction. *J Mol Biol* **356:** 142–154.

Lai, Z.B., Li, Y., Wang, F., Cheng, Y., Fan, B.F., Yu, J.Q., and Chen, Z.X. (2011) Arabidopsis sigma factor binding proteins are activators of the WRKY33 transcription factor in plant defense. *Plant. Cell* **23:** 3824–3841.

Lee, Y.H., and Dean, R.A. (1993) cAMP regulates infection structure formation in the plant pathogenic fungus *Magnaporthe grisea*. *Plant. Cell* **5:** 693–700.

Levin, D.E. (2011) Regulation of cell wall biogenesis in *Saccharomyces cerevisiae*: the cell wall integrity signaling pathway. *Genetics* **189:** 1145–1175.

Li, G., Zhou, X., and Xu, J.R. (2012) Genetic control of infection-related development in *Magnaporthe oryzae*. *Curr Opin Microbiol* **15:** 678–684.

Li, G., Zhou, X., Kong, L., Wang, Y., Zhang, H., Zhu, H., *et al*. (2011) MoSfl1 is important for virulence and heat tolerance in *Magnaporthe oryzae*. *PLoS One* **6:** e19951.

Li, J.J., and Xie, D. (2015) RACK1, a versatile hub in cancer. *Oncogene* **34:** 1890–1898.

Li, L., Xue, C.Y., Bruno, K., Nishimura, M., and Xu, J.R. (2004) Two PAK kinase genes, CHM1 and MST20, have distinct functions in *Magnaporthe grisea*. *Mol Plant Microbe Interact* **17:** 547–556.

Liu, W., Zhou, X., Li, G., Li, L., Kong, L., Wang, C., *et al*. (2011) Multiple plant surface signals are sensed by different mechanisms in the rice blast fungus for appressorium formation. *PLoS Pathog* **7:** e1001261.

Mayorga, M.E., and Gold, S.E. (2001) The ubc2 gene of *Ustilago maydis* encodes a putative novel adaptor protein required for filamentous growth, pheromone response and virulence. *Mol Microbiol* **41:** 1365–1379.

Melamed, D., Bar-Ziv, L., Truzman, Y., and Arava, Y. (2010) Asc1 supports cell-wall integrity near bud sites by a Pkc1 independent mechanism. *PLoS One* **5:** e11389.

Mentlak, T.A., Kombrink, A., Shinya, T., Ryder, L.S., Otomo, I., Saitoh, H., *et al*. (2012) Effector-mediated suppression of chitin-triggered immunity by *Magnaporthe oryzae* is necessary for rice blast disease. *Plant Cell* **24:** 322–335.

Mitchell, T.K., and Dean, R.A. (1995) The cAMP-dependent protein kinase catalytic subunit is required for appressorium formation and pathogenesis by the rice blast pathogen *Magnaporthe grisea*. *Plant Cell* **7:** 1869–1878.

Mosquera, G., Giraldo, M.C., Khang, C.H., Coughlan, S., and Valent, B. (2009) Interaction transcriptome analysis identifies *Magnaporthe oryzae* BAS1-4 as biotrophy-associated secreted proteins in rice blast disease. *Plant Cell* **21:** 1273–1290.

Motoyama, T., Ochiai, N., Morita, M., Iida, Y., Usami, R., and Kudo, T. (2008) Involvement of putative response regulator genes of the rice blast fungus *Magnaporthe oryzae* in osmotic stress response, fungicide action, and pathogenicity. *Curr Genet* **54:** 185–195.

Motoyama, T., Kadokura, K., Ohira, T., Ichiishi, A., Fujimura, M., Yamaguchi, I., and Kudo, T. (2005) A two-component histidine kinase of the rice blast fungus is involved in osmotic stress response and fungicide action. *Fungal Genet Biol* **42:** 200–212.

Park, G., Xue, C., Zheng, L., Lam, S., and Xu, J.R. (2002) MST12 regulates infectious growth but not appressorium formation in the rice blast fungus *Magnaporthe grisea*. *Mol Plant Microbe Interact* **15:** 183–192.

Park, G., Xue, C., Zhao, X., Kim, Y., Orbach, M., and Xu, J.R. (2006) Multiple upstream signals converge on the adaptor protein Mst50 in *Magnaporthe grisea*. *Plant Cell* **18:** 2822–2835.

Rachfall, N., Schmitt, K., Bandau, S., Smolinski, N., Ehrenreich, A., Valerius, O., and Braus, G.H. (2013) RACK1/Asc1p, a ribosomal node in cellular signaling. *Mol Cell Proteomics* **12:** 87–105.

Ramezani-Rad, M. (2003) The role of adaptor protein Ste50-dependent regulation of the MAPKKK Ste11 in multiple signalling pathways of yeast. *Curr Genet* **43:** 161–170.

Reynolds, N., and Ohkura, H. (2003) Polo boxes form a single functional domain that mediates interactions with multiple proteins in fission yeast polo kinase. *J Cell Sci* **116:** 1377–1387.

Saunders, D.G., Dagdas, Y.F., and Talbot, N.J. (2010a) Spatial uncoupling of mitosis and cytokinesis during appressorium-mediated plant infection by the rice blast fungus *Magnaporthe oryzae*. *Plant Cell* **22:** 2417–2428.

Saunders, D.G., Aves, S.J., and Talbot, N.J. (2010b) Cell cycle-mediated regulation of plant infection by the rice blast fungus. *Plant Cell* **22:** 497–507.

Schamber, A., Leroch, M., Diwo, J., Mendgen, K., and Hahn, M. (2010) The role of mitogen-activated protein (MAP) kinase signalling components and the Ste12 transcription factor in germination and pathogenicity of *Botrytis cinerea*. *Mol Plant Pathol* **11:** 105–119.

Thines, E., Weber, R.W.S., and Talbot, N.J. (2000) MAP kinase and protein kinase A - dependent mobilizationof triacylglycerol and glycogen during appressorium tugor generation by *Magnaporthe grisea*. *Plant Cell* **12:** 1703–1718.

Truckses, D.M., Bloomekatz, J.E., and Thorner, J. (2006) The RA domain of Ste50 adaptor protein is required for delivery of Ste11 to the plasma membrane in the filamentous growth signaling pathway of the yeast *Saccharomyces cerevisiae*. *Mol Cell Biol* **26:** 912–928.

Villalba, F., Collemare, J., Landraud, P., Lambou, K., Brozek, V., Cirer, B., *et al*. (2008) Improved gene targeting in *Magnaporthe grisea* by inactivation of MgKU80 required for non-homologous end joining. *Fungal Genet Biol* **45:** 68–75.

Wang, G., Li, G., Zhang, S., Jiang, C., Qin, J., and Xu, J.R. (2015) Activation of the signalling mucin MoMsb2 and its functional relationship with Cbp1 in *Magnaporthe oryzae*. *Environ Microbiol* **17:** 2969–2981.

Wang, L., Berndt, P., Xia, X., Kahnt, J., and Kahmann, R. (2011) A seven-WD40 protein related to human RACK1 regulates mating and virulence in *Ustilago maydis*. *Mol Microbiol* **81:** 1484–1498.

Wilson, R.A., and Talbot, N.J. (2009) Under pressure: investigating the biology of plant infection by *Magnaporthe oryzae*. *Nat Rev Microbiol* **7:** 185–195.

Xu, J.R., and Hamer, J.E. (1996) MAP kinase and cAMP signaling regulate infection structure formation and pathogenic growth in the rice blast fungus *Magnaporthe grisea*. *Genes Dev* **10:** 2696–2706.

Xu, J.R., Staiger, C.J., and Hamer, J.E. (1998) Inactivation of the mitogen-activated protein kinase Mps1 from the rice blast fungus prevents penetration of host cells but allows activation of plant defense responses. *Proc Natl Acad Sci U S A* **95:** 12713–12718.

Xu, J.R., Urban, M., Sweigard, J.A., and Hamer, J.E. (1997) The CPKA gene of *Magnaporthe grisea* is essential for appressorial penetration. *Mol Plant Microbe Interact* **10:** 187–194.

Yi, M., Chi, M.H., Khang, C.H., Park, S.Y., Kang, S., Valent, B., and Lee, Y.H. (2009) The ER chaperone LHS1 is involved in asexual development and rice infection by the blast fungus *Magnaporthe oryzae*. *Plant Cell* **21:** 681–695.

Yin, Z., Tang, W., Wang, J., Liu, X., Yang, L., Gao, C., *et al*. (2015) Phosphodiesterase MoPdeH targets MoMck1 of the conserved mitogen-activated protein (MAP) kinase signalling pathway to regulate cell wall integrity in rice blast fungus *Magnaporthe oryzae*. *Mol Plant Pathol* **17:** 654–668.

Yu, J.H., Hamari, Z., Han, K.H., Seo, J.A., Reyes-Dominguez, Y., and Scazzocchio, C. (2004) Double-joint PCR: a PCR-based molecular tool for gene manipulations in filamentous fungi. *Fungal Genet Biol* **41:** 973–981.

Yuan, L., Su, Y., Zhou, S., Feng, Y., Guo, W., and Wang, X. (2017) A RACK1-like protein regulates hyphal morphogenesis, root entry and in vivo virulence in *Verticillium dahliae*. *Fungal Genet Biol* **99:** 52–61.

Zhai, C., Li, K., Markaki, V., Phelan, J.P., Bowers, K., Cooke, F.T., and Panaretou, B. (2008) Ypp1/YGR198w plays an essential role in phosphoinositide signalling at the plasma membrane. *Biochem J* **415:** 455–466.

Zhang, S., and Xu, J.R. (2014) Effectors and effector delivery in *Magnaporthe oryzae*. *PLoS Pathog* **10:** e1003826.

Zhao, X.H., Kim, Y., Park, G., and Xu, J.R. (2005) A mitogen-activated protein kinase cascade regulating infection-related morphogenesis in *Magnaporthe grisea*. *Plant Cell* **17:** 1317–1329.

Zheng, W., Zhao, Z.Y., Chen, J.S., Liu, W.D., Ke, H.Y., Zhou, J., *et al*. (2009) A Cdc42 ortholog is required for penetration and virulence of *Magnaporthe grisea*. *Fungal Genet Biol* **46:** 450–460.

Zhou, X., Li, G., and Xu, J.R. (2011) Efficient approaches for generating GFP fusion and epitope-tagging constructs in filamentous fungi. *Methods Mol Biol* **722:** 199–212.

Zhou, X., Zhang, H., Li, G., Shaw, B., and Xu, J.R. (2012) The Cyclase-associated protein Cap1 is important for proper regulation of infection-related morphogenesis in *Magnaporthe oryzae*. *PLoS Pathog* **8:** e1002911.

Zhou, X., Zhao, X., Xue, C., Dai, Y., and Xu, J.R. (2014) Bypassing both surface attachment and surface recognition requirements for appressorium formation by overactive ras signaling in *Magnaporthe oryzae*. *Mol Plant Microbe Interact* **27:** 996–1004.

Supporting information

Additional Supporting Information may be found in the online version of this article at the publisher's website:

Fig. S1. Mst50-3xFLAG construct was functional in *M. oryzae*.
Fig. S2. Western blot analysis with the anti-Mst50 antibody.
Fig. S3. TEY phosphorylation assays with the *chm1* mutant and the *mst20* mutant.
Fig. S4. Phenotypes of the *mck1* mutant.
Fig. S5. Increased sensitivity of the *mst50* mutant to hydrogen peroxide.
Fig. S6. The *MIP11* gene replacement and deletion mutants.
Fig. S7. The *MIP17* genomic region and phenotypes of the *mip17* mutant.
Table S1. PCR primers used in this study.
Table S2. Phenotypic characterization of the *mip17* mutant in *M. oryzae*.